Research Article J. Electrochem. Sci. Technol., 2017, 8(3), 244-249

Journal of Electrochemical Science and Technology
jecst.org

Analysis of the Singular Point of Cyclic Voltammograms Recorded with Various Scan Rates

Byoung-Yong Chang*
Department of Chemistry, Pukyong National University, 45 Yongso-ro, Nam-gu, Busan 608-739, Korea

ABSTRACT

This paper presents the results of an investigation into the *isoamperic* point of cyclic voltammograms, which is defined as the singular point where the voltammograms of various scan rates converge. The origin of the unique point is first considered from a theoretical perspective by formulating the voltammetric curves as a system of linear equations, the solution of which indicates that a trivial solution is only available at the potential at which the net current is zero during the reverse potential scan. In addition, by way of a mathematical formulation, it was also shown that the isoamperic point is dependent on the switching potential of the potential scanning. To validate these findings, theoretical and practical cyclic voltammmograms were studied using finite-element based digital simulations and 3-electrode cell experiments. The new understanding of the nature of the isoamperic point provides an opportunity to measure the charge transfer effects without the influence of the mass transfer effects when determining the thermodynamic and kinetic characteristics of a faradaic system.

Keywords : Cyclic voltammogram, Theoretical electrochemistry, Finite element simulation

Received : 16 June 2017, Accepted : 17 August 2017

1. Introduction

Singular points that are associated with multiple curves are sometimes observed in chemical measurements, and indicate information of interest. In spectroscopy, the isosbestic point is found at a specific wavelength (or wavenumber, frequency) where multiple spectra converge to a constant absorbance value [1]. When a system undergoes chemical or physical changes that result in an isosbestic point, this unchanging point can be used as a reference point to evaluate the progress of those changes [2]. Another frequently observed singular point is the isoelectric point at which the positive and negative charge curves intersect before the net charges eventually become zero [3]. When molecular or colloidal particles have charges on their surface, this isoelectric point can play a critical role in describing the changes in their chemical or physical behaviors. By monitoring this point, the potential, migration, solubility, and functionality of biomaterials can be controlled [4-5].

In electrochemistry, a similar singular point is found for potentials that change with temperature [6]. According to the Nernst equation, the electrode potential changes linearly relative to the logarithm of the concentrations of redox chemicals, and the slope of the changes is determined by the temperature. However, when the same amounts of redox chemicals are present in the solution, the electrode potential is always the same regardless of temperature. Thus, the isothermal point where the changing potential curves converge is a singular point of potential. For instance, a pH meter has this isothermal point at pH = 7, which is utilized for self-calibration or error correction purposes [7-8].

Another interesting singular point is observed in cyclic voltammograms. Cyclic voltammetry is the most frequently used technique for electroanalytical purposes, and records the electrochemical current during potential scans under controlled conditions. Traditionally, once an optimized potential range has

*E-mail address: bychang@pknu.ac.kr
DOI: https://doi.org/10.5229/JECST.2017.8.3.244

been determined, the scan rate is varied to determine the specific parameter values of interest. For example, if the electrochemical reaction is controlled by the diffusion of redox species, the current is proportional to the square-root of the scan rate [9-10], whereas if it is bound to the electrode surface, the current is directly proportional to the scan rate [11-12]. The behaviors of these linear curves provide insight into the kinetic and thermodynamic information. Even though a *cyclic* voltammogram consists of both forward and reverse sections, the forward section is well studied while the reverse section is not, except for the case of finding the reversibility of a faradaic reaction. This is because the reverse current is produced differently from the switching potential of the scan. Because of this, the true value of the peak current for the reverse scan must be obtained by correcting the measured value using a specific equation. To accomplish this, our group recently reported a more accurate equation that can be used to mathematically correct the current variations [13].

By overlaying the cyclic voltammograms of different scan rates, we observe a very distinctive point where all the cyclic voltammograms converge, as shown in Fig. 1. It is noteworthy that this *singular* point can be observed regardless of the scan rate and switching potential, which indicates that it can provide unique information with regard to reduction-oxidation processes. However, even though this point shows up frequently, to the best of my knowledge, it has not been the subject of any reports in the literature. To rectify this, in this article, I provide the results of my investigation into the meaning of this singular point.

2. Experimental

2.1 Simulation

Theoretical cyclic voltammograms were obtained using the finite element method (FEM). As the method is well described elsewhere [13-14], it is only described briefly here. With the assumption that the solution is fully electrolyzed by the inert and supporting electrolytes, only the Ox and Red species are considered when calculating the mass transfer, and the concentrations are denoted $C_O(d, t)$ and $C_R(d, t)$ at a certain distance (d) from the electrode at a certain time (t). These values were incorporated into the FEM simulation as digitized $C_O(n, m)$ and $C_R(n, m)$

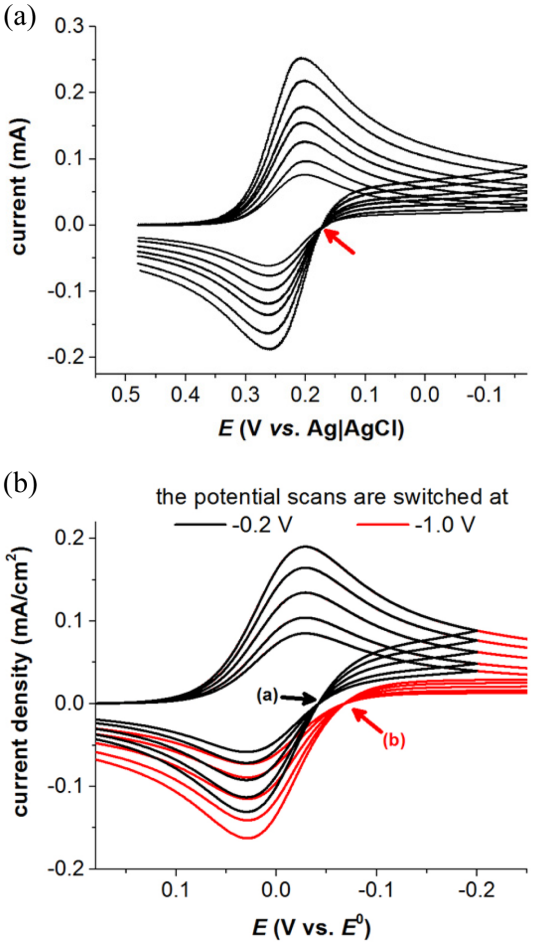

Fig. 1. (a) Cyclic voltammograms of $Fe(CN)_6^{3-/4-}$ were recorded at scan rates of 20, 30, 50, 75, 100, 150, and 200 mV/s. The other experimental conditions are described in the Experimental section. The singular point is indicated by the red arrow. (b) Theoretical cyclic voltammograms obtained by FEM simulation with scan rates of 20, 30, 50, 75, and 100 mV/s. The black and red curves were obtained when the potential scans were reversed at -0.20 and -1.0 V vs. $E^{0'}$, and the singular points of each curve set are indicated by the respective arrows. To simplify the display, only a portion of the cyclic voltammograms for -1.0 V are shown.

values in a 2D-matrix as dimensionless parameters defined by $n = d / \Delta d$, and $m = t / \Delta t$, respectively. All calculations were conducted in MATLAB®.

Conventionally, the rate of mass transfer is balanced with that of the charge transfer at the interface of the electrode, and is presented as the flux of the Ox and Red species. The digitized flux of the finite ele-

ments is calculated using the following equation with dimensionless parameters k_f and k_b as the charge transfer rate constants describing the forward and backward reactions and D_M as the mass transfer diffusion coefficient.

$$-J(m) = \frac{k_f C_O(1, m) - k_r C_R(1, m)}{(1 + k_f/2D_M + k_r/2D_M)}, \quad (1)$$

On the other hand, in the bulk solution, only the diffusion of the Ox and Red species are considered and calculated using Fick's first and second laws. The application of those laws to dimensionless elements is accomplished using the following equation, after which the values are stored in the matrix and applied to Eq. (1).

$$C(n, m+1) = C(n, m) + D_M[C(n-1, m) - 2C(n, m) + C(n+1, m)] \quad (2)$$

Finally, $J(m)$ in Eq. (3) is re-dimensionlized by multiplying by $\Delta d/\Delta t$ to construct a voltammogram.

2.2 Cyclic voltammetry experiments

In these experiments, an electrochemical cell is configured with working, counter, and reference electrodes that are Pt plate and a home-made Ag|AgCl, respectively. The electrolyte solution consists of doubly distilled water containing 5.0 mM of ferricyanide (Sigma Aldrich) as the electroactive species and 100 mM of KNO_3 (Sigma Aldrich) as the supporting electrolyte. The electrochemical experiments were performed using a commercial potentiostat (SP200, Bio-Logic Science Instruments, France). The cyclic voltammograms were recorded at a scan rate of 20 to 200 mV/s and the potential scans were switched to reverse at 0.0 to -500 mV *vs*. Ag|AgCl.

2.3 Theoretical considerations

The key outstanding question for the singular point is why the voltammetric curves formed by different scan rates converge at a particular potential-current point. Under conventional electrochemical experimental conditions, the mass transfer is dominated by the diffusion of the redox species when there are sufficient supporting electrolytes, and the charge transfer is due to the electrode potential. A combination of charge and mass transfers in a certain amount of measurement time produces a voltammogram. When an electrochemical reaction is reversible with rapid charge transfer, the faradaic current is determined by the rate of mass transfer by diffusion, which can be formulated as follows:

$$i = nFAD\frac{C^* - C_{x=0}}{L}, \quad (3)$$

where n is the number of electrons transferred, F is the faradaic constant, A is the electrode area, D is the diffusion coefficient, C^* is the bulk concentration, $C_{x=0}$ is the surface concentration, and L is the diffusion length, which is equal to $L = \sqrt{2Dt}$.

When the potential (E) changes with time (t), then $E = E_{int} - \nu t$, and Eq. (3) becomes

$$i(E, \nu) = nFAD\frac{C^* - C_{x=0}}{\sqrt{2D(E_{int} - E)}}\sqrt{\nu} \quad (4)$$

In a reversible system, $C_{x=0}$ is only determined by E; thus, Eq. (4) can be simplified into a function of E and ν. The following equation is a variation of Eq. (3) with separate variables:

$$i(E, \nu) = X(E)\sqrt{\nu} \quad (5)$$

Here, $X(E)$ can be clearly expressed as a closed form of mathematical equation for the forward scan, but this is not possible for the reverse scan as that requires numerical analyses. Many experimental results in the literature have proven that $i(E, \nu)$ is linearly related to $\sqrt{\nu}$ for both forward and reverse scans, even without an exact evaluation of $X(E)$ [10, 14]. Thus, Eq. (5) can be empirically validated, and was also proven by the theoretical simulation data in Fig. 1.

Equation (5) implies that $i(E, \nu)$ cannot be the same for different values of ν, except $X(E) = 0$. This is a trivial solution for the system of linear equations in Eq. (5), which describe multiple E and ν values. In other words, in order to ensure the voltammetric current values converge to a certain value regardless of $\sqrt{\nu}$, $X(E)$ should be 0, which means that the singular point is now determined by a specific potential. As $X(E)$ is non-zero for the forward scan, we can determine the singular point for the backward scan. Here, we conclude that the singular point appears when the reverse scan current is zero. This conclusion can be intuitively derived from Nicholson and

Shain's approach in which they plotted theoretical cyclic voltammograms while calculating the semi-integration equations describing the dimensionless parameters [15]. A practical cyclic voltammogram can be obtained by multiplying $\sqrt{\nu}$ with the dimensionless one. This approach results in Eq. (5), which indicates that the singular point is only obtained by the trivial solution. At this singular point, the overall faradaic reaction changes from reduction to oxidation or *vice versa*. This will be discussed in the context of the switching potential scan. Note that both approaches rely on the assumption that the current is only due to the faradaic reactions. If there are non-faradaic processes involved, they will cause the singular points to float, which is beyond the scope of the present report.

3. Results and Discussion

As can be seen in Fig. 1(a), the different cyclic voltammograms converge to a singular point potential, at which the currents are constant regardless of the scan rate while the voltammetric currents are strongly dependent on the scan rates. As explained above, the isoamperic potential, which is the potential of the singular point of voltammograms, is found to be a trivial solution for the linear equations in Eq. (5), which renders the scan rate term ineffective. Even though we have identified the origin of the singular point, we still do not know what electrochemical information it represents because this point stands alone and does not control the electrochemical parameters, such as the scan rate, diffusion coefficient, concentrations of redox species, transfer coefficient (α), and so on. The singular point is independent of the rates of potential scans, but is dependent on the range of potential scans.

As shown in Fig. 2, it can be seen that that the singular points at the isoamperic potential (E_{iso}) change with the switching potential (E_λ) during experiments. As the switching potentials E_λ become more negative in a reduction reaction, E_{iso} also increases; however, no quantitative relationship can be observed between E_λ and E_{iso} in Fig. 2(b).

In order to determine the correlation between these values, simulations were conducted to obtain theoretical cyclic voltammograms to discover values of E_{iso} that were changed by E_λ. As shown in Fig. 3, a linear relationship was found when $\Delta E_\lambda / \Delta E_{iso}$ was plotted versus E_λ. Eventually, linear curve fitting results in

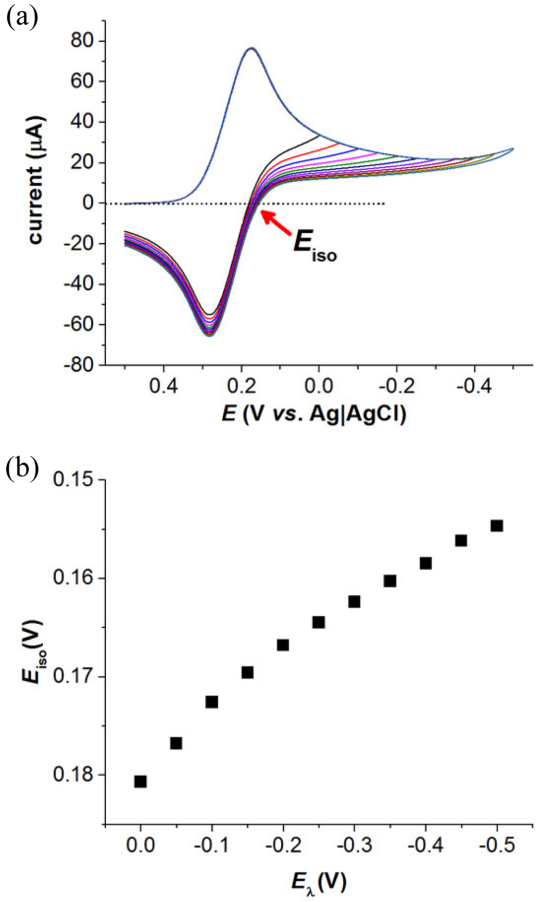

Fig. 2. (a) Cyclic voltammograms of $Fe(CN)_6^{3-/4-}$ were recorded at scan rates of 20 mV/s, and the potential scans were switched to reverse between E_λ = 0.00 through -0.50 V vs. Ag|AgCl. The E_{iso} values of each scan rate were acquired with respect to E_λ. (b) Plot of E_{iso} along E_λ.

the following relationship:

$$\frac{dE_\lambda}{dE_{iso}} = -73.53(E_\lambda - E^{0'} + 0.0565) \quad (6)$$

Solving this differential equation leads to:

$$-E_{iso} = 0.0138\ln(-E_\lambda + E^{0'} - 0.0565) + \beta \quad (7)$$

where β is an integration constant that can be determined by numerical analyses on simulation data or measured by experiments. Considering $E^{0'}$ and the number of electrons (n), the following equation applies:

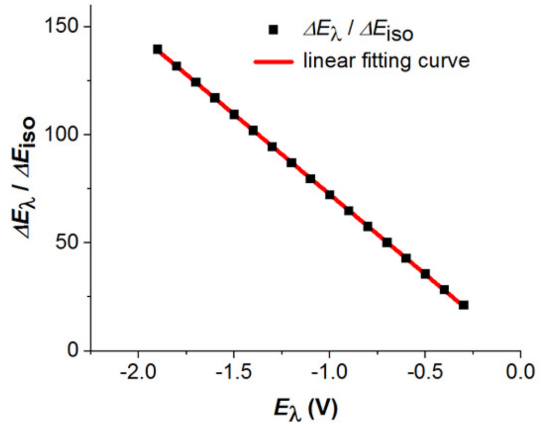

Fig. 3. Plot of $\Delta E_\lambda / \Delta E_{iso}$ along E_λ, together with its linear fitting curve (solid red line).

$$-E_{iso} = \frac{0.0138}{n}\ln\left(-E_\lambda + E^{0'} - \frac{0.0565}{n}\right) + \beta_n - E^{0'}, \quad (8)$$

when the reverse potential scan activates the oxidation reaction, while

$$E_{iso} = \frac{0.0138}{n}\ln\left(E_\lambda - E^{0'} + \frac{0.0565}{n}\right) - \beta_n + E^{0'} \quad (9)$$

applies when the reverse potential scan activates the reduction reaction with $\beta_1 = 0.0685$, $\beta_2 = 0.0390$, and $\beta_3 = 0.0278$ according to n. Note that the +/- signs are switched to make the value positive inside the logarithm along with the other parameters. Also, as the number in the logarithm should be positive, those equations suggest that the overpotential for potential scan switches is larger than $E^{0'}$ by at least 0.0565 / n. Fig. 4(a) shows plots of E_{iso} resulting from simulations of cyclic voltammograms with different values of n, of which the linear fitting curves are exactly the same as those in Eq. (8) that were derived theoretically. Also, the values of E_{iso} that were experimentally measured from the cyclic voltammograms in Fig. 2(a) are plotted in Fig. 4(b) and fitted to a linear curve. Upon investigation, the slope was found to be 0.0138 with an intercept of 0.0543 - $E^{0'}$, which is very close to the theoretical values of 0.0138 and 0.0685 - $E^{0'}$, respectively. All of the simulation and experimental results strongly support the linear relationship between E_{iso} and the modified E_λ for Eq. (5).

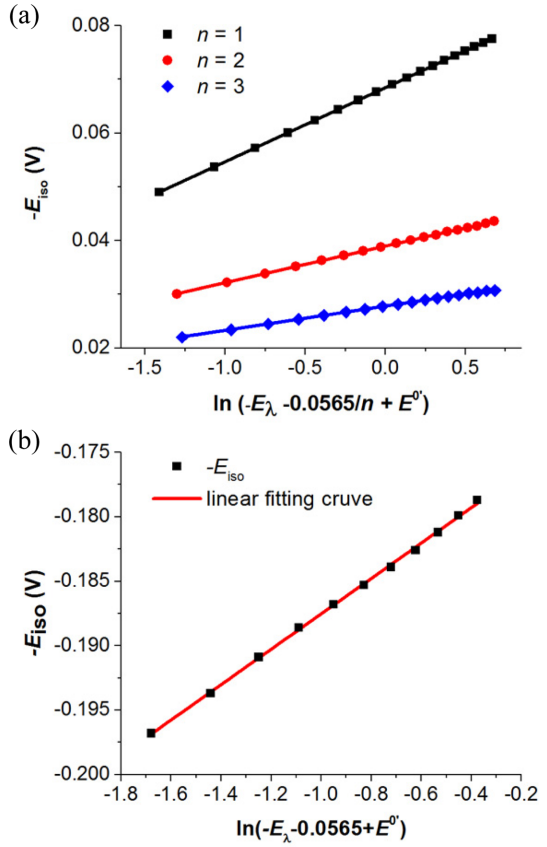

Fig. 4. (a) Plots of -E_{iso} along the calculated values of ln (−E_λ − 0.0565/n + $E^{0'}$). The values E_{iso} are obtained from the simulation results of cyclic voltammograms with n = 1, 2 and 3, respectively. Linear fits are carried out for each data set, and result in a slope of 0.0138/n. (b) Plots of -E_{iso} along the values of ln (−E_λ − 0.0565/n + $E^{0'}$). Here, the values of E_{iso} and E_λ were experimentally measured from cyclic voltammograms of Fig. 2(a). The linear fitting curve has a slope of 0.0138 and an intercept of 0.0543 − $E^{0'}$, which are very close to the theoretical values of 0.0138 and 0.0685 - $E^{0'}$.

4. Conclusions

It has long been observed that the cyclic voltammograms of a reversible electrochemical reaction converge on a singular point when they are recorded with different scan rates. As is well known, the electrochemical current is proportional to the square-root of the scan rate, and the voltammetric curve can therefore be formulated as a function of potential-dependent and scan rate-dependent sections, respectively. In this paper, for a common value of current, a

system of linear equations was solved to yield a trivial solution, and the trivial solution was when the potential-dependent part was zero at a certain potential, which is referred to as the *isoamperic* point. At the isoamperic potential, the current changes from reductive to oxidative states, or *vice versa*, and should be observed when the direction of the potential scan is reversed. Consequently, the potential when the potential scan is switched is important. Based on the simulation results, the isoamperic potential was found to have a logarithmic relationship with the switching potential.

Despite discovering the origin of the singular point of cyclic voltammograms, the significance of the isoamperic point is still not clear. All that is known is that the faradaic reactions switch from reductive to oxidative states or *vice versa* at this point. Nevertheless, an area of future work is to acquire the thermodynamic and kinetic information that pertain to this point. As the current at the isoamperic point is zero, the mass transfer effect can be neglected. Consequently, the charge transfer is only observable without being influenced by the mass transfer at the solution/electrolyte interface. Conditions with either no or controlled mass transfer effects are very convenient for electrochemical impedance spectroscopy experiments, as the Nyquist plot shows clear semicircles of resistance with no interference from the straight line of the Warburg impedance [16-18].

Acknowledgment

This research was supported by a Research Grant of Pukyong National University (2015).

References

[1] John W. Moore, Ralph G. Pearson, *Kinetics and Mechanism*, *3rd Ed*., Wiley, **1981**, 48-51.
[2] M. Greger, M. Kollar and D. Vollhardt, *Physical Review B*, **2013**, *87(19)*, 195140.
[3] H.J. Cleaves, *Isoelectric Point In Encyclopedia of Astrobiology*, Springer Berlin Heidelberg, (2011) 858-859.
[4] B. Bjellqvist, G.J. Hughes, C. Pasquali, N. Paquet, F. Ravier, J.-C. Sanchez, S. Frutiger and D. Hochstrasser, *ELECTROPHORESIS*, **1993**, *14(1)*, 1023-1031.
[5] M. Son, D. Kim, J. Kang, J.H. Lim, S.H. Lee, H.J. Ko, S. Hong and T.H. Park, *Analytical Chemistry*, **2016**, *88(23)*, 11283-11287.
[6] D. Midgley, *Analyst,* **1987**, *112(5)*, 573-579.
[7] S. Bhadra, D.S.Y. Tan, D.J. Thomson, M.S. Freund and G.E. Bridges, *IEEE Sensors Journal.*, **2013**, *13(6)*, 2428-2436.
[8] D. Midgley, *Analyst*, **1987**, *112(5)*, 581-585.
[9] S. Hong, H. Jo and S.-W. Song, *J. Electrochem. Sci. Technol.*, **2015**, *6*, 116-120.
[10] S.O.R. Siadat, *J. Electrochem. Sci. Technol*, **2015**, *6(4)*, 111-115.
[11] I. Kang, W.-S. Shin, S. Manivannan, Y. Seo and K. Kim, *J. Electrochem. Sci. Technol*, **2016**, *7*, 277-285.
[12] A.F.T. Auguste, G.C. Quand-Meme, K. Ollo, B. Mohamed, S.S. placide, S. Ibrahima and O. Lassiné, *J. Electrochem. Sci. Technol.*, **2016**, *7(1)*, 82-89.
[13] B.-Y. Chang, *J. Electrochem. Sci. Technol.*, **2016**, *6*, 146-151.
[14] S.-H. Oh and B.-Y. Chang, *J. Electrochem. Sci. Technol.*, **2016**, *7*, 293-297.
[15] R.S. Nicholson and I. Shain, *Analytical Chemistry*, **1964**, *36(4)*, 706-723.
[16] S.-H. Kang, S.-Y. Lee, J.-H. Kim, C.-J. Choi, H. Kim and K.-S. Ahn, *J. Electrochem. Sci. Technol.*, **2016**, *7*, 52-57.
[17] M. Aliaghayee, H.G. Fard and A. Zandi, *J. Electrochem. Sci. Technol*., **2016**, *7*, 218-227.
[18] E.K. Park and J.W. Yun, *J. Electrochem. Sci. Technol.*, **2016**, *7*, 33-40.